Tunable Low-Rate Genomic Recombination with Cre-lox in *E. coli*: A Versatile Tool for Synthetic Biology and Environmental Sensing

Elisa Garabello[1], Hyun Yoon[1,2], Matthew C. Reid[1], Andrea Giometto[1*]

1. School of Civil and Environmental Engineering, Cornell University, Ithaca, NY 14853, USA
2. Department of Civil and Environmental Engineering, University of California, Berkeley, CA 94720, USA

ABSTRACT

A variety of synthetic biology applications, from environmental sensing to bioproduction, would benefit from the ability to induce genomic alterations at low, tunable rates. Site-specific recombinases can be used to perform a variety of targeted DNA modifications such as excisions, inversions, and integrations. Their specificity and efficiency are offset by leaky expression and challenges in engineering a dynamic range of recombination rates. Here, we developed a tightly regulated, titratable Cre recombinase system that is tailored to achieve low recombination rates in *Escherichia coli*. As a proof-of-concept application of this design, we developed a whole-cell recombination-based arsenic biosensor, with detection sensitivity comparable to traditional wet chemical methods. Furthermore, our biosensor allows decoupling exposure from measurement, which could benefit assays in more complex, realistic settings. This system enables targeted genetic recombination events at experimentally tunable rates with application in ecological, environmental and cell physiology research, and beyond.

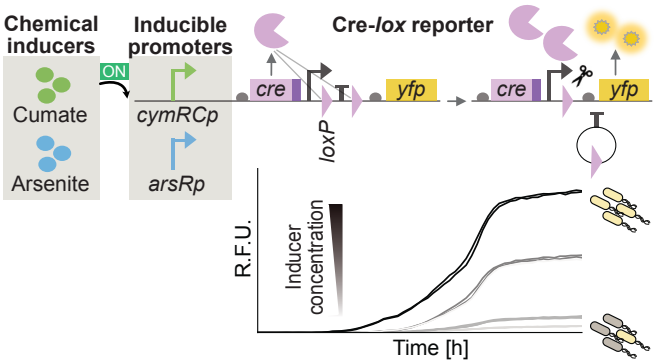

INTRODUCTION

Engineered microbiological systems are enabling significant advances across a diverse range of fields, including industrial applications in the pharmaceutical and energy sectors, as well as in ecological, environmental, and cell physiology research.[1] The convergence of DNA sequencing, gene editing techniques, and rational modeling of genetic components as modular and standardized parts of a circuit is advancing the construction of increasingly sophisticated and robust systems. Prominent components of this toolkit are site-specific recombinases and nucleases that enable alterations to the genome *in vivo* at specific loci. These modifications can be used to induce reversible or irreversible phenotypic changes and are trackable using reporter systems such as fluorescent proteins. Among these DNA modifying enzymes, Cre is a tyrosine

recombinase able to recombine with high specificity and efficiency two short sequences, called *lox* sites. If the *lox* sites are oriented in the same 5' to 3' direction in the same DNA molecule, Cre excises the DNA contained between them.[2,3] The Cre recombinase can perform various other types of genetic recombination, such as DNA inversion, integration, and translocation, expanding the range of genetic circuits in which it can be used. The new genotype is inherited by daughter cells and is maintained even after Cre expression is interrupted. This feature, shared by other recombinases such as Flp and Bxb1, has been exploited in synthetic genetic logic gates and circuits with a memory component.[4,5] Unlike nucleases such as CRISPR-Cas systems, recombinases can autonomously perform excision and genetic recombination without relying on the cell's double-strand break repair systems. This characteristic may offer an advantage in organisms like *Escherichia coli*, where DNA repair options, though varied, predominantly depend on homology-directed mechanisms that may be less efficient or more error-prone.

Many genetic constructs employing a recombinase system enclose a transcriptional terminator between the recombinase recognition sites, so that the downstream gene is silenced until the recombinase is expressed and the terminator is removed via recombinase-mediated excision. This can constitute a binary switch at the single-cell level that can be regulated by outside triggers or by tissue-specific promoters, often engineered to generate a rapid and swift transition of the population into a new genotypic state. While less attention has been dedicated to developing genetic constructs that constrain Cre activity at low recombination rates, engineering such a titratable Cre-*lox* system would enable dynamic control of a population phenotypic state distribution, as demonstrated recently by Williams *et al*.[6] for Bxb1-mediated recombination. Successful applications of Cre-*lox* systems in eukaryotic hosts such as yeast, plants and mice differ significantly in their regulation mechanism with respect to bacteria. For example, in the Mother Enrichment Program in yeast[7], Cre is fused with a nuclear receptor ligand and is constitutively expressed and sequestered in the cytoplasm, until intracellular β-estradiol mediates its transport into the nucleus. On the other hand, in bacteria, recombinases have direct access to the attachment sites on the genome packed in the nucleoid. This poses challenges to a tight regulation of the recombinase activity, which is necessary to limit baseline expression and tune recombination rates experimentally. To control Cre recombinase activity in bacteria, Sheets *et al.*[8] constructed and characterized different variants of an optogenetic system that regulates it at the post-translational level. Although using a light signal to regulate Cre expression brings benefits such as temporal control over recombination activity, it also limits the experimental setup which can be employed, due to the necessity to control sample illumination at all times.

Here, we developed and characterized titratable Cre-*lox* reporters with low background expression in *E. coli*. This was achieved by regulating Cre recombinase expression at the transcriptional level and controlling Cre stability post-translationally. These constructs can be plasmid-based or chromosomally-integrated and are designed to induce phenotypic switches at low, chemically-inducible rates. This makes them suitable for a range of uses beyond traditional synthetic biology applications, such as metabolic engineering, and extends to experiments in cell physiology, ecology, and evolutionary biology.

We demonstrate the broad applicability of these constructs by developing a Cre-recombinase-based biosensor for quantification of bio-available arsenite. Arsenic (As) is a widespread environmental contaminant that significantly affects both human health and ecological systems. The chemical speciation, transport, and fate of arsenic are influenced by microbial activities, and understanding these processes is crucial for studying its biogeochemical cycling.[9] Trivalent arsenite (As(III)) is particularly prevalent in anaerobic environments such as waterlogged rice paddies and groundwater aquifers, in which mobilization of arsenic presents a threat to human health. We compare our system with respect to more established transcription-based fluorescent reporters and discuss the benefits of the former.

RESULTS AND DISCUSSION

This section is organized as follows. First, we describe the optimization of Cre-*lox* constructs for titratable, low-rate recombination by expressing *cre* from a promoter inducible by 4-Isopropylbenzoic acid (cuminic acid). Second, we characterize the inducer response of these constructs at both the population and single-cell levels. Third, we discuss the development of a Cre-recombinase-based arsenite biosensor. Finally, we examine the broader applicability of our constructs.

Aiming to reduce and control Cre activity, our first construct mounted on a low copy number plasmid (pEG36, origin or replication *pA15*) expressed *cre* from the cumate sensitive promoter *cymRCp* obtained from the "Marionette" sensors collection.[10,11] This promoter is repressed by the regulator $CymR^{AM}$ (constitutively expressed from the chromosome of the host strain, sAJM.1504[10]) in the absence of cumate. Both $cymR^{AM}$ and *cymRCp* are mutated with respect to wild-type to provide lower leakage and increased dynamic range. In addition, pEG36 includes $cymR^{AM}$, which maintains the ratio between the copy numbers of the regulator $cymR^{AM}$ and the promoter *cymRCp* close to one. Finally, we added the C-terminal *ssrA-LVA* degradation tag[12] to the *cre* gene to reduce the Cre half-life in the cell and thus its activity (Fig. 1).

To test the inducer-response curve of this circuit and other variants, we assembled a construct composed of a constitutive promoter, two transcriptional terminators flanked by two *loxP sites* (part of phage P1's wild-type Cre-*loxP* system) with the same orientation, followed by the enhanced yellow fluorescent protein gene (*eyfp*). In the presence of both *loxP* sites, the two transcriptional terminators terminate transcription, leaving *eyfp* unexpressed (Fig. 1A). Upon Cre-induced recombination of the two *loxP* sites, the transcriptional terminators are excised (Fig. 1B), enabling expression of the fluorescent protein that we detected using a fluorescence plate reader or a flow cytometer, depending on the assay. Simultaneous measurements of optical density at 600 nm (OD600) and fluorescence at the plate reader allowed us to identify cumate concentrations that did not significantly affect growth rates (Table S1), while promoting strong Cre activity.

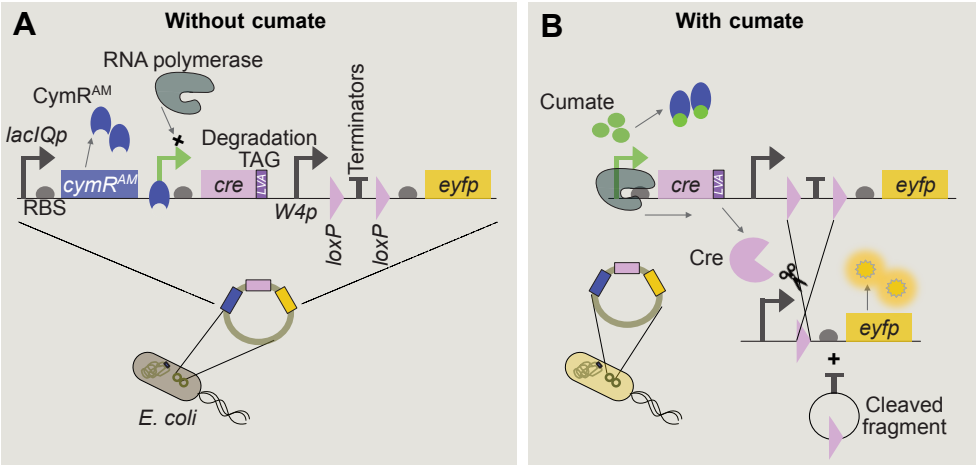

Fig. 1. Schematic of the Cre-*loxP* reporter system in *E. coli* on a plasmid. (A) In the absence of cumate, the constitutively expressed repressor CymR^{AM} occupies the *cymRCp* operator site, inhibiting *cre* transcription. (B) When cumate is present, it binds to the repressor, which detaches from the operator site allowing *cre* transcription. If the *loxP* sites are positioned in the same orientation, Cre excises the terminators located between the *loxP* sites and transcription of *eyfp* is initiated.

Fig. 2A shows that pEG36 has low leakage and titratable Cre activity across a reproducible range. To further vary the titratability range of the construct, we tested different regulatory strategies at both the transcriptional and the post-translational level (Fig. 2). Specifically, we explored the possibility of altering the activity of our low-rate Cre-*loxP* system by adopting heterologous *lox* sites (pAG56), by removing the Cre degradation tag (not shown), or by reducing the gene copy number of *cymR^{AM}* by removing it from the plasmid (pEG39). We observed a dramatic drop in the fraction of fluorescent cells in the population, and thus in Cre activity, when the first wild-type *loxP* was replaced with *lox511* (Fig. 2B), which differs from *loxP* by a single point mutation.[13,14] Although we were able to obtain higher fractions of fluorescent cells by inducing this construct with concentrations of cumate higher than the upper limit we had set, this had a sizable fitness cost (Table S1). Since this construct had a reduced titratability range compared to other variants, we did not characterize it further, but it may be of interest for longer assays, for example for growth in a chemostat, in which recombination of homologous *lox* sites constructs such as pEG36 would likely reach saturation (100% fluorescent cells) in a short time. Removal of the Cre degradation tag resulted in frequent recombination even in the absence of the inducer, making it impossible to obtain clonal populations with two intact *loxP* sites, unless heterologous *lox* sites were used (data not shown). Conversely, recombination rates increased, as expected, when *cymR^{AM}* was removed from the plasmid (pEG39, Fig. 2C), leaving only the chromosomal copy. This may be of interest for applications that require a reporter with high sensitivity and quick response times. The various plasmids variants are listed in Table 1.

After constructing the plasmids described above and characterizing their inducer-response curves, we integrated the Cre-*loxP* reporter sequence with homologous *loxP* sites from pEG55 into the chromosome at *attTn7* (bEG57). This sequence differs from pEG39 by substituting *eyfp* with the yellow super fluorescent protein gene *syfp2* and using a stronger promoter and ribosome binding site to increase the fluorescence signal. Chromosomal integration guarantees a more

homogeneous gene copy number in the population and longer stability of the Cre-*loxP* reporter construct across generations, even in the absence of selective agents.

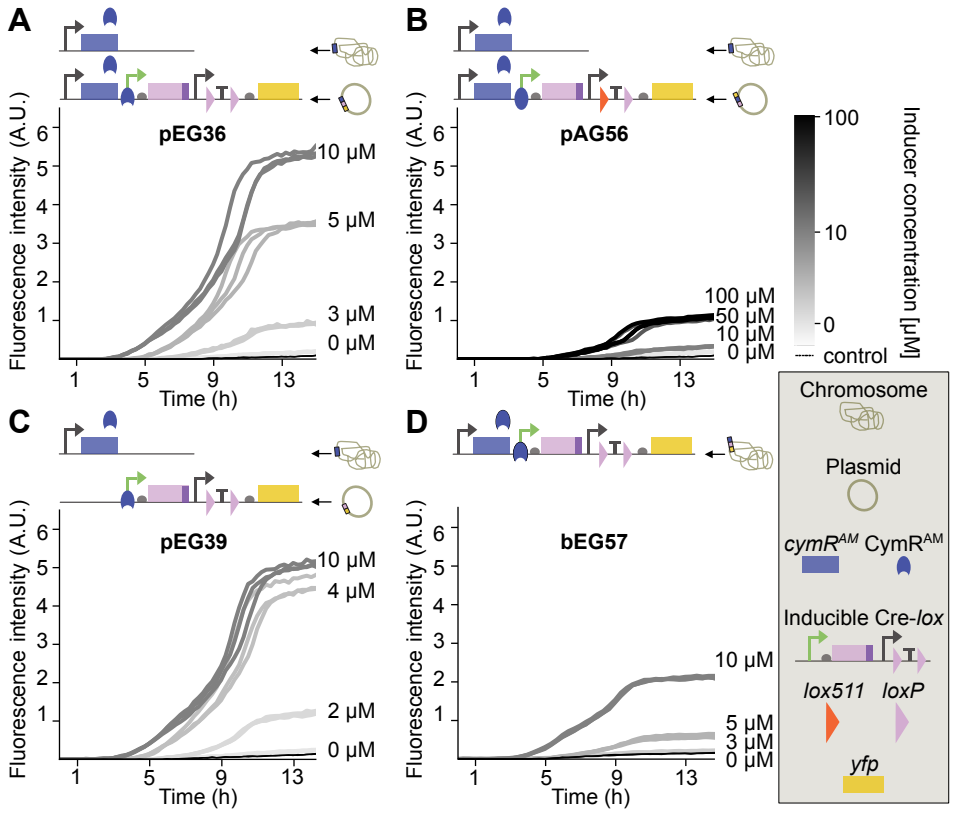

Fig. 2. Inducer-response curves of four Cre-*lox* reporter variants measured at the plate reader. The fluorescence intensity and range of titratability of the reporters varied depending on the copy number of the repressor gene *cymR*^{AM} (A vs C), on the identity of *lox* sites (homologous in A vs heterologous in B), and on the genomic location of the circuit (plasmid in A vs chromosome in D). Each curve shows a different technical replicate. The negative control is the fluorescence intensity recorded for the parent strain Marionette-Clo which contains a copy of *cymR*^{AM} on the chromosome and neither a Cre-*lox* circuit nor *eyfp*.

We decided to further characterize reporters of interest (pEG36 and bEG57) at the single-cell level using flow-cytometry, as we reasoned that it would allow us to detect recombination events earlier than with the fluorescence plate reader. To capture the kinetics of these reporters, we collected samples of the cell population during both the exponential and stationary phases at various time points (Fig. 3A). Cytometry measurements allowed us to carry out a high-throughput analysis of the fraction of cells expressing the fluorescence reporter and to observe fluorescence heterogeneity at the single cell level (Fig. 3C), even when the population fluorescence was well below the detection limit of the plate reader. In addition, we performed colony PCR of each sample, amplifying the region enclosing the *loxP* sites. This allowed us to identify via gel electrophoresis and Sanger sequencing whether these samples contained DNA corresponding to the original (two *loxP*) or the recombined (one *loxP)* sequences, or a mix of the two (Fig. 3D). We identified plasmid pEG36 (with *cymR*^{AM} and two *loxP*) as a good candidate to quantitatively characterize the response of the reporter, due to the range of titratability we could explore by employing reasonably low concentrations of inducer. Both pEG36 and pEG39 (two *loxP*, no

cymR^{AM}) can reach saturation of cells which cut the *loxP* site in a single growth-curve by adding 10 μM of cumate, however pEG36 shows slower recombination rates than pEG39, allowing us to follow the reporter kinetics taking measurements at more widely spaced time points. Together with pEG36, we characterized the chromosomally integrated reporter bEG57. We considered pEG36 to be the ideal plasmid reporter to compare with the chromosomal Cre-*loxP* reporter, due to the approximately equal ratio between gene copy numbers of the repressor and of Cre expressed by the cumate-sensitive promoter. To estimate recombination rates (Fig. 3B), we fit flow-cytometry data in the exponential growth phase with a simple deterministic model (Methods) that assumes a constant recombination rate during the exponential growth phase.

Table 1 | Summary of relevant plasmids and strains used in this study

Strain	**Source**	**Genotype**
sAJM.1504	Meyer *et al.*[10]	*E. coli* Marionette-Clo (DH10B background), *cymR*^{AM} on chromosome
bEG57	This work	sAJM.1504; *attTn7*::*cymRCp – cre*-LVA, *rpsLp – loxP – TT – loxP – syfp2*
Plasmid	**Source**	**Key Inserts**
pAJM.657	Meyer *et al.*[10]	*cymR*^{AM}, *cymRCp – eyfp*
pAG56	This work	*cymR*^{AM}*, cymRCp – cre-LVA, W4p – lox511 – TT – loxP – eyfp*
pEG36	This work	*cymR*^{AM}*, cymRCp – cre-LVA, W4p – loxP – TT – loxP – eyfp*
pEG39	This work	*cymRCp – cre-LVA, W4p – loxP – TT – loxP – eyfp*
pEG55	This work	*cymRCp – cre-LVA, rpsLp – loxP – TT – loxP – syfp2*
pMP01	Pothier *et al.*[15]	ArsRBS2 – *mCherry* (pUCP19 backbone)
pEG69	This work	ArsRBS2 – *cre-LVA, rpsLp – loxP – TT – loxP – syfp2*
pEG78	This work	ArsRBS2 – *syfp2*
Units	**Source**	**Genetic Elements**
TT	Chen *et al.*[16]	Transcriptional terminators *ECK120033736 – L3S2P11*
ArsRBS2	Pothier *et al.*[15]	*arsRBS – arsRp – arsR – arsRBS*

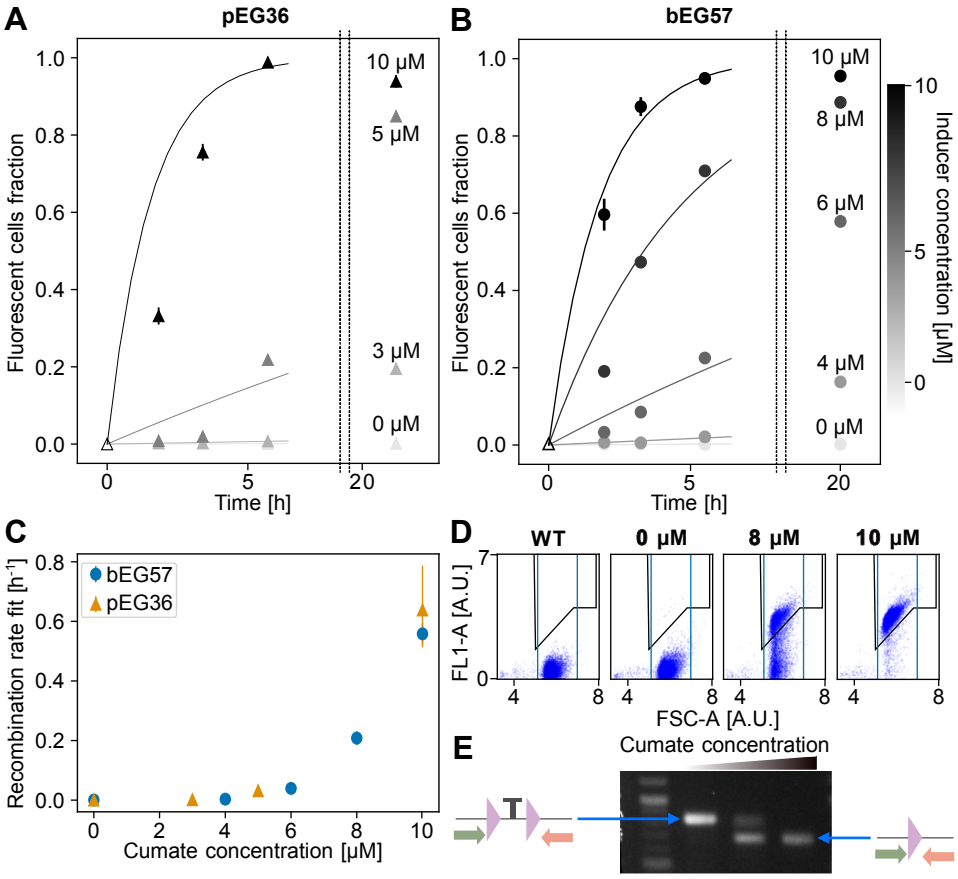

Fig. 3. Inducer-response curves measured at the flow-cytometer for the low-rate Cre-*loxP* reporter systems on plasmid pEG36 (with *cymR*^{AM} and two *loxP*) and on the chromosome, bEG57. (A-B) Fraction of fluorescent cells in the population with the plasmid (A) or chromosomal (B) reporter. Each point is the average of 3 technical replicates; error bars report the SEM. Time point 0 h is the same for all treatments and is the fraction of fluorescent cells in the starting culture after exiting the lag phase and before adding the inducer. Lines represent the deterministic recombination model fitted to the data within the exponential phase. (C) Best-fit of the recombination rate parameter (Eq. 1) with respect to the inducer concentration; error bars are the SD of the parameter estimate. (D) Example of collected flow-cytometry data; scatterplots of the fluorescence intensity signal area (FL1-A) vs forward-scattered area (FSC-A) for each single-cell for chromosomal reporter samples. Threshold gates are shown as blue lines (for the FSC-A channel) and black polygons (for FL1-A). (E) Gel electrophoresis of PCR products resulting from the amplification of the region enclosing the *loxP* sites. Brightness was adjusted to highlight both bands.

To demonstrate the applicability of these designs for environmental sensing, we built a proof-of-concept Cre-*loxP* reporter in which *cre* transcription is induced by arsenite. To this end, we expressed both *cre* and *E. coli*'s transcriptional repressor *arsR* from the *arsRp* promoter in a bicistronic design (pEG69). We refer to this reporter as ArsRBS2-Cre-*loxP*-SYFP2, where ArsRBS stands for ArsR Binding Site, and the number 2 highlights that, following Stocker *et al.*,[17] we introduced an auxiliary copy of ArsRBS before the *cre* gene to reduce leakage, in addition to the ArsRBS before *arsR* (Fig. 4A). We grew this recombinase-based arsenite reporter with concentrations of As(III) as low as 15 nM, comparable to the sensitivity of existing whole-cell arsenic biosensors and wet-chemical methods including inductively coupled plasma mass spectrometry (ICP-MS).[18] To compare the sensitivity of our recombinase-based reporter pEG69

to that of a transcription-based reporter, we used a modified version of the plasmid reporter pMP01 from Pothier *et al.*,[15] ArsRBS2-SYFP2, carrying *syfp2* instead of *mCherry*, with the same backbone as pEG69 (Fig. 4B). Unlike ArsRBS2-SYFP2 where *syfp2* transcription is regulated via the promoter *arsRp*, expression of *syfp2* in ArsRBS2-Cre-*loxP*-SYFP2 is regulated by a strong, constitutive promoter. To compare the two biosensors, we took endpoint, single-cell fluorescence measurements at the flow-cytometer for both reporters, grown with arsenite concentrations from 0 to 60 nM. Since the transcription-based reporter returns a continuous response, we took the median single-cell fluorescence intensity as the representative measure of the overall expression level. On the other hand, we observed limited leakage in ArsRBS2-Cre-*loxP*-SYFP2, with an increase in the fraction of fluorescent cells in the population of 0.091%±0.006% (mean±SEM) in the assay without arsenite. We expected some basal expression due to the negative feedback loop. For comparison, in the treatments with added arsenite, the fraction of fluorescent cells ranged from 0.157%±0.007% to 0.66%±0.01%, corresponding to the minimum and maximum inducer concentration, respectively. We found that both the ArsRBS2-Cre-*loxP*-SYFP2 and ArsRBS2-SYFP2 reporters could detect 15 nM arsenite (p-value < 0.01), which is lower than the EPA threshold values for arsenic contamination in drinking water (10 ppb As or ~80 nM As).[18] Unlike ArsRBS2-SYFP2, the Cre-recombinase based biosensor maintains a memory of arsenite exposure, allowing the user to decouple exposure from measurement. This is an advantage over existing anaerobic biosensor methods which require all aspects of the experiment, including plate reader fluorescence measurements, to be performed inside an anaerobic chamber.[19,20]

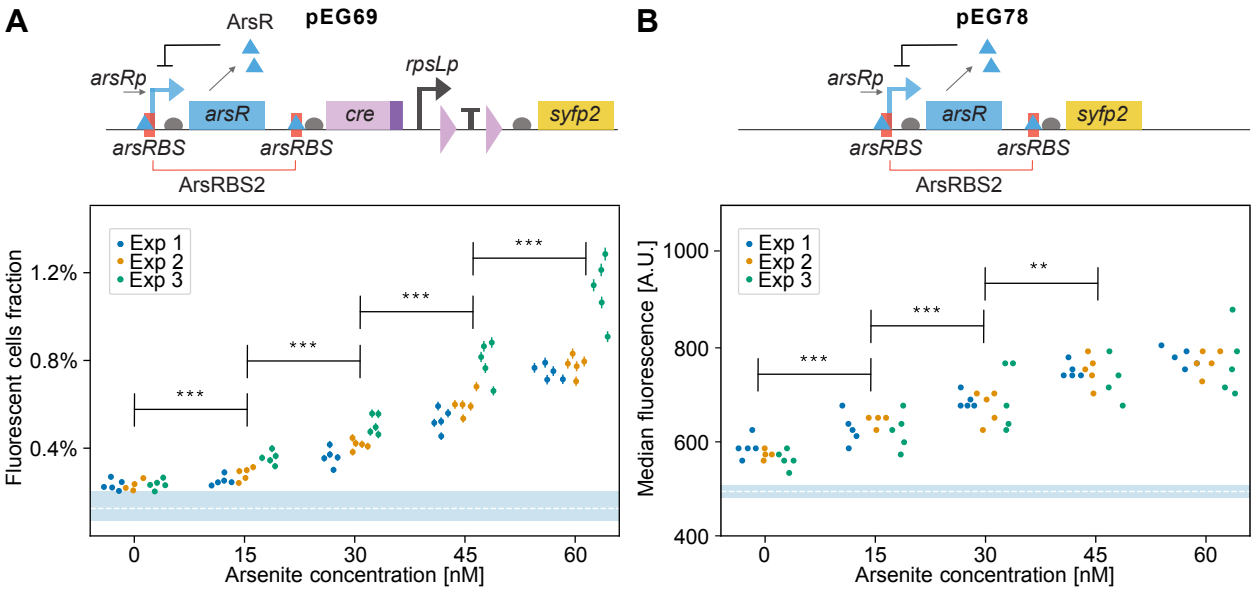

Fig. 4. Schematics of the arsenite whole-cell biosensors and endpoint fluorescence measurements collected at the flow-cytometer. (A) Recombinase-based biosensor schematics (top) and fraction of fluorescent cells at the end of the assay (bottom; error bars report the Poisson counting error). (B) Transcription-based biosensor schematics (top) and median cell fluorescence in each sample (bottom; error bars computed via bootstrapping are smaller than symbols). In both panels, each point is a technical replicate, for the three biological replicates shown with different colors. The light blue regions report the minimum and maximum values of the fraction of fluorescent cells (A) or median cell fluorescence (B) at the start of the experiment before induction with arsenite, while the white dashed line represents the intermediate measured value. Experiment 3 (green symbols) lasted an hour longer (18 vs 17 hours) with

respect to the two other replicates, which might explain the larger fraction of fluorescent cells compared to the other two experiments. Note that due to different designs, the measured response is different depending on the bioreporter: for the recombinase-based biosensor we report on the y-axis the fraction of fluorescent cells, counted by cytometry gating; for the transcription-based reporter we report the median cell fluorescence intensity.

To summarize, in this work we first explored how different regulatory strategies of a Cre-*lox* system affect the response of a cumate-inducible reporter in *E. coli*. We observed that the use of an optimized inducible promoter and protein degradation tag effectively limits leakage. Furthermore, we showed that recombination rates can be manipulated by changing the ratio of gene copy numbers of the regulator and transcriptional promoter, and that extremely low recombination rates can be achieved by hindering Cre activity by substituting homologous *loxP* sites with the heterologous *lox511*-*loxP* pair. Mutated Cre recombinases[21] with lower recombination efficiency could be further employed to build reporters with different titratability ranges. The constructs developed here provide an alternative to optogenetic Cre-*loxP* systems[8] and only necessitate low concentrations of a chemical, cuminic acid, that is inexpensive and unharmful to cells. Moreover, the dynamic range of induction could be further manipulated by supplementing the growth medium with salicylic acid, which antagonizes the cumate reporter.[10]

Recombinases have been largely employed in synthetic biology applications leveraging their efficiency, specificity and ability to create a genetic memory. Titratable recombinase systems pose additional challenges in prokaryotic compared to eukaryotic hosts, in particular for efficient recombinases like Cre, because a tight regulation of their activity is required to prevent uninduced modifications of the genome in the absence of a nucleus. Being able to experimentally tune recombinase-mediated recombination rates *in vivo* across a titratable range may find applications in genetic circuit design,[6] cell physiology[7] and microbial ecology and evolution[22] research.

To demonstrate the broad applicability of our circuits, we used the same design principle of our optimized cumate-inducible Cre-*loxP* constructs to develop a recombinase-based arsenite biosensor. The majority of existing whole-cell arsenite biosensors[15,17] adopt traditional designs comprising fluorescence-based reporter circuits in which transcription of a fluorescent protein is regulated by the *arsRp* promoter. Our biosensor's capability to detect recombination events at small rates could be particularly useful for monitoring arsenic pollution in real-world environments, such as rice paddies, where microbial uptake of dissolved arsenic can be inhibited due to factors including complexation with dissolved organic matter, association with colloidal phases, or repression of arsenic uptake by organic carbon.[20,23] In the future, the reporter construct could be further optimized to reduce leakage, for example by disrupting the *arsR* negative feedback loop,[24] or using an engineered version of the *arsRp* promoter.

Biogeochemical interactions between arsenic, iron, and sulfur that govern arsenic chemical speciation and fate depend strongly on redox conditions, highlighting the need for experimental methods to characterize microbial availability of arsenite under anaerobic conditions where it is most mobile, as found for example in waterlogged paddy soils, wetlands, marine sediments, and deep subsurface environments. Although the use of flavin-based fluorescent proteins allows traditional biosensor designs to function in anoxic or anaerobic assays,[19,20] the high signal-to-

noise ratio of these measurements can significantly reduce the sensitivity and accuracy of detecting low concentrations of analytes. In contrast, recombinase-based biosensors, such as the one developed here, are particularly suitable for these assays thanks to the decoupling of environmental sensing from measurements. This genetic memory brings interesting new functionalities compared to traditional biosensors and can be advantageous for obtaining temporally-integrated measurements in the field or laboratory,[25] with cells transitioning to the recombined state at low rates over extended periods of time. Although the development of recombinase-based environmental biosensors is still relatively limited in the literature,[26] their potential to address these challenges makes them a promising tool for environmental sensing.

MATERIALS AND METHODS

Strain editing

We assembled and characterized the cumate reporter in the Marionette-Clo *E. coli* strain,[10] which has DH10B background. On plasmids, *eyfp* transcription is controlled by the constitutive, medium-strength promoter *W4p*.[8] In the chromosomal reporter, *syfp2*[10,27] transcription is regulated by the high-strength constitutive promoter *rpsLp*. *rpsLp-syfp2* was amplified from strain eDE31, which was a gift from Johan Paulsson. Cre was a gift from Niels Geijsen (Addgene plasmid # 62730). The terminators *ECK120033736 and L3S2P11* and mutant *lox* sites were synthesized by Twist Bioscience. *loxP* and *W4p* were a gift from Mary Dunlop (Addgene plasmid # 134405). Plasmids were constructed using FastCloning[28] or Gibson assembly[29]. Oligos used are reported in Table S3. Chromosomal insertions were achieved via the mTn7 (MCS MS26) mobile element, inserting at *attTn7*, downstream of *glmS*, following the protocol in Sibley & Raleigh.[30] Plasmids were isolated with the Omega Bio-Tek E.Z.N.A. Plasmid DNA Mini Kit I (Q - spin) and sequenced via Oxford Nanopore long-read sequencing. Chromosomal insertions were amplified with primers oAG70/oEG103 (Table S3) surrounding *attTn7* and sequenced via Oxford Nanopore long-read sequencing. After substituting *mCherry* in pMP01 with the Cre-*loxP*-SYFP2 construct (Fig. 4A), we moved the reporter sequence on a vector with low copy number (*pA15* origin of replication). This significantly decreased the leakage of the reporter. The ArsRBS2-Cre-*loxP* and ArsRBS2-SYFP2 constructs were assembled via Fastcloning, except for the last step, consisting in swapping the backbone with a low copy number vector, which was performed via enzymatic restriction cloning.

Media and chemical inducers

Characterization of the cumate-inducible constructs was performed in Lysogeny Broth (LB) medium with the appropriate selective antibiotic, whereas the arsenite-inducible constructs characterization was done in MOPS for growth medium (MPG), following the recipe used in Pothier *et al.*,[31] supplemented with 50 µg/µL ampicillin. Super Optimal broth with Catabolite repression (SOC) medium and plates made with Lysogeny Broth (LB) medium with 1.5% agar and 50 µg/µL kanamycin were used for cloning and strain maintenance. Unless specified otherwise, cells were grown in LB with the appropriate selective antibiotic. To induce *cre* transcription, we added appropriate amounts of a stock solution of 100 mM cuminic acid (4-Isopropylbenzoic acid) ≥ 96% purity (Sigma-Aldrich 268402) in 100% ethanol to the medium. The

arsenite bioreporter strains were grown in MOPS for growth medium (MPG), following the recipe used in Pothier *et al.*[31]

Cumate-sensitive reporter response characterization

Plate reader assays: Overnights of strains of interest were grown from fresh single colonies on agar at 37 °C in 1 mL of LB in a roller drum. The following day, cultures were diluted 1:200 in glass culturing tubes and incubated at 37 °C on the roller drum for 2 hours. Afterwards, cells were further diluted 1:100 in pre-warmed LB with antibiotic and inducer and, for each sample and treatment, a total of 1.5 mL was distributed in equal volumes of 125 µL into 12 wells of a sterile, flat-bottom, non-treated, 96-well tissue culture plate with lid (VWR 10861-562). Three technical replicates were used for each treatment condition and time-step recovery. The samples were distributed on the plate in a random configuration. Cells were then grown in the plate reader at 37 °C with continuous double orbital shaking at 807 cpm. Strains were induced with a range of cumate concentrations ranging from 0 µM to the maximum concentration of cumate as recommended in Meyer *et al.*,[10] i.e. 100 µM. OD600 and fluorescence (excitation at 501 nm and emission at 533 nm) were measured every 15 minutes over 21 hours of incubation. OD600 and fluorescence data of 3 wells inoculated with only medium and no cells were averaged at each timestep and used as a measure of background expression. At four time points, after 1 h, 2 h 30 min, 5 h and 21 h from the beginning of the assay, the plate was shortly removed from the plate reader, between 2 and 5 µL were transferred from each well into a volume ranging from 125 to 198 µL of Tris-HCl pH 7.5 in a 96-well U bottom plate to perform flow-cytometry measurements (10,000 single cells recorded per sample).

Flow-cytometry and colony PCR: Flow-cytometry was performed by collecting forward and side scattering (FSC/SSC), as well as fluorescence intensity with excitation at 488 nm and emission at 533±15 nm (FL1-A). Three wells for each treatment were pooled and used as template for colony PCRs to amplify the DNA region enclosing the two *loxP* sites. After qualitatively comparing the bands length difference, the DNA was purified from the PCR product with the Omega Bio-Tek E.Z.N.A. Cycle Pure Kit (V-Spin) and Sanger sequenced. The generated chromatograms were analyzed to measure the abundance of nucleotide variants. In all experiments, the parent strain Marionette-Clo was used as a negative control and Sanger sequenced. The generated chromatograms were analyzed to measure the abundance of nucleotide variants. In all experiments, the parent strain Marionette-Clo was used as a negative control.

Recombination rate analysis

We use a simple, deterministic model, to quantitatively describe the population dynamics and quantify the *Cre* recombination rate. The model variables are:

- $n_{not_rec}(t)$: number of cells that did not undergo Cre recombination, and thus are not expressing the fluorescent protein.
- $n_{rec}(t)$: number of cells which underwent recombination and are thus expressing the fluorescent protein.
- $N(t) = n_{rec}(t) + n_{not_rec}(t)$: total population size. Estimated via an OD_{600} – cell density calibration curve prepared beforehand.

- μ: growth rate
- K: carrying capacity.

The model assumes:

1. Same growth rate μ for n_2 and n_1.
2. Recombination events taking place at constant rate κ during the exponential growth phase.
3. No recombination events in stationary phase.

We can then write

$$\frac{dn_{not_rec}}{dt} = \mu n_{not_rec}\left(1 - \frac{n_{rec} + n_{not_rec}}{K}\right) - \kappa n_{not_rec}$$
$$\frac{dn_{rec}}{dt} = \mu n_{rec}\left(1 - \frac{n_{rec} + n_{not_rec}}{K}\right) + \kappa n_{not_rec}$$

and derive the equation describing the fraction of cells with 1 *loxP* site:

$$f = \frac{n_{rec}}{N} = 1 - e^{-\kappa t}. \quad (1)$$

Here, we are not taking into consideration the fluorescence protein expression dynamics, but only considering the changes in the genetic composition of the population. The "effective" recombination rate estimated from the reporter inducer-response curves measured at the flow-cytometer is likely affected by a delay factor due to the fluorescence protein maturation time. To fit Eq. (1) to our data, for each treatment, we performed a linear fit of $\ln(1 - f)$ versus time, with zero intercept, to the average fraction of fluorescent cells across technical replicates.

Arsenite sensitive reporter response characterization and analysis

A stock solution of 7 mM of arsenite was prepared by dissolving sodium arsenite (LabChem, Zelienople, PA) in Milli-Q water, followed by 0.22 µm syringe-filtration. The preparation was conducted in a Coy anaerobic chamber (98% N_2 and 2% H_2), and the stock solution was stored anaerobically at 4°C after its concentration was verified using inductively coupled plasma mass spectrometry (ICP-MS; Agilent 7800). Negligible oxidation of arsenite to arsenate was confirmed prior to use by high-performance liquid chromatography (HPLC; Agilent 1260 Infinity) hyphenated to ICP-MS. From this stock, we collected 15 µL diluted in a total volume of 15 mL sterile water in a 15 mL falcon tube. Experiments were carried out in the same week the 70 µM arsenite stock was prepared, to minimize the solution exposure to the air and the risk of oxidation into As(V). Yoon *et al.*[32] verified the absence of arsenite speciation in their biosensor experiments via HPLC-ICP-MS analysis, with sampling conducted during the first 10 hours of their experiment.[32]

The host strain used for the arsenite biosensors is *E. coli* NEB 10-beta, which has DH10B background. Strains used for the arsenite sensitive reporter assay were streaked from the cryostock on an LB agar plate with 2% dextrose with 50 µg/mL kanamycin and 50 µg/mL ampicillin and incubated at 37 °C overnight. At least 3 colonies per strain were picked and inoculated in 2 mL-deep 96 well plates (VWR 76397-576) with 1 mL of MPG supplemented with 50 µg/mL ampicillin and 100 µL of 20% dextrose. The plate was covered with a rayon film and lid and placed on an orbital shaker rotating at 400 rpm in a 37 °C incubator. The following day, samples were measured at the flow cytometer. Dextrose helped reduce Cre expression leakage, probably due

its inhibitory action on the glycerol facilitator transporter protein (GlpF), which mediates the uptake of arsenite by the cell.[23] The biological replicates with the least leakage were selected for the assay. Cells were washed in MPG to remove glucose and diluted 10,000 fold in MPG with ampicillin and different concentrations of arsenite. Technical replicates were inoculated in 2 mL-deep 96-well plates and kept in the incubator with 400 rpm orbital shaking until they reached stationary phase. Samples were measured at the flow cytometer after 17 hours of incubation (18 hours for the third biological replicate) by sampling between 10 and 12 μL of liquid, which were then diluted in 50 mM Tris-HCl pH 7.5. For each well, we collected 150,000 single-cell measurements. The binary response of the recombinase-based biosensor was measured at the single cell level by measuring the fraction of cells contained within a gate in the FSC-A vs FL1-A that was drawn by comparing cells grown in the absence of As(III) to fully-recombined cells.

To assess statistical significance (p-value < 0.05) of the sensors' sensitivity, within the same biological replicate, we performed two-sided Welch's t-tests between treatments at successive inducer concentrations (i.e., 0 nM with 15 nM, 15 nM with 30 nM, etc). The p-values obtained from the three different experiments (biological replicates) for the same arsenite concentration were then combined following Fisher's method. The corresponding p-values are reported in Table S2.

ACKNOWLEDGEMENTS

We thank Andrew Murray for insightful comments on the manuscript and Katie Randolph for help with the experiments. AG acknowledges support by the National Institute of General Medical Sciences of the National Institutes of Health, United States of America under award number 1R35GM147493. MCR acknowledges support from NSF grant 1905175.

CORRESPONDENCE

*Andrea Giometto, School of Civil and Environmental Engineering, Cornell University, Ithaca, NY 14853, USA. Email: giometto@cornell.edu.

SUPPORTING INFORMATION

Supporting information include supplementary tables reporting strains' growth rates measured in the experiments carried out to characterize the cumate-sensitive reporter population, p-values of all statistical tests performed, the main oligonucleotides used in this study, and additional notes on data analyses.

BIBLIOGRAPHY

1. Shams, A., Fischer, A., Bodnar, A. & Kliegman, M. Perspectives on Genetically Engineered Microorganisms and Their Regulation in the United States. ACS Synth. Biol. 13, 1412–1423 (2024).
2. Hoess, R. H. & Abremski, K. Mechanism of strand cleavage and exchange in the Cre-lox site-specific recombination system. J. Mol. Biol. 181, 351–362 (1985).
3. Tian, X. & Zhou, B. Strategies for site-specific recombination with high efficiency and precise spatiotemporal resolution. J. Biol. Chem. 296, 100509 (2021).
4. Siuti, P., Yazbek, J. & Lu, T. K. Synthetic circuits integrating logic and memory in living cells. Nat.

Biotechnol. 31, 448–452 (2013).
5. Hsiao, V., Hori, Y., Rothemund, P. W. & Murray, R. M. A population-based temporal logic gate for timing and recording chemical events. Mol. Syst. Biol. 12, 869 (2016).
6. Williams, R. L. & Murray, R. M. Integrase-mediated differentiation circuits improve evolutionary stability of burdensome and toxic functions in E. coli. Nat. Commun. 13, 6822 (2022).
7. Lindstrom, D. L. & Gottschling, D. E. The mother enrichment program: a genetic system for facile replicative life span analysis in Saccharomyces cerevisiae. Genetics 183, 413–22, 1SI–13SI (2009).
8. Sheets, M. B., Wong, W. W. & Dunlop, M. J. Light-Inducible Recombinases for Bacterial Optogenetics. ACS Synth. Biol. 9, 227–235 (2020).
9. Zhu, Y.-G., Yoshinaga, M., Zhao, F.-J. & Rosen, B. P. Earth Abides Arsenic Biotransformations. Annu. Rev. Earth Planet. Sci. 42, 443–467 (2014).
10. Meyer, A. J., Segall-Shapiro, T. H., Glassey, E., Zhang, J. & Voigt, C. A. Escherichia coli 'Marionette' strains with 12 highly optimized small-molecule sensors. Nat. Chem. Biol. 15, 196–204 (2019).
11. Choi, Y. J. et al. Novel, versatile, and tightly regulated expression system for Escherichia coli strains. Appl. Environ. Microbiol. 76, 5058–5066 (2010).
12. Andersen, J. B. et al. New unstable variants of green fluorescent protein for studies of transient gene expression in bacteria. Appl. Environ. Microbiol. 64, 2240–2246 (1998).
13. Siegel, R. W., Jain, R. & Bradbury, A. Using an in vivo phagemid system to identify non-compatible loxP sequences. FEBS Lett. 505, 467–473 (2001).
14. Missirlis, P. I., Smailus, D. E. & Holt, R. A. A high-throughput screen identifying sequence and promiscuity characteristics of the loxP spacer region in Cre-mediated recombination. BMC Genomics 7, 73 (2006).
15. Pothier, M. P., Hinz, A. J. & Poulain, A. J. Insights Into Arsenite and Arsenate Uptake Pathways Using a Whole Cell Biosensor. Front. Microbiol. 9, 2310 (2018).
16. Chen, Y.-J. et al. Characterization of 582 natural and synthetic terminators and quantification of their design constraints. Nat. Methods 10, 659–664 (2013).
17. Stocker, J. et al. Development of a set of simple bacterial biosensors for quantitative and rapid measurements of arsenite and arsenate in potable water. Environ. Sci. Technol. 37, 4743–4750 (2003).
18. Bhat, A., Hara, T. O., Tian, F. & Singh, B. Review of analytical techniques for arsenic detection and determination in drinking water. Env. Sci. Adv. (2023) doi:10.1039/d2va00218c.
19. Hinz, A. J., Stenzler, B. & Poulain, A. J. Golden Gate Assembly of Aerobic and Anaerobic Microbial Bioreporters. Appl. Environ. Microbiol. 88, e0148521 (2022).
20. Yoon, H. et al. Effects of iron and dissolved organic matter on bioavailability of arsenite under anaerobic conditions. ACS ES T Water 3, 3676–3686 (2023).
21. Hartung, M. & Kisters-Woike, B. Cre mutants with altered DNA binding properties. J. Biol. Chem. 273, 22884–22891 (1998).
22. Wahl, M. E. & Murray, A. W. Multicellularity makes somatic differentiation evolutionarily stable. Proc. Natl. Acad. Sci. U. S. A. 113, 8362–8367 (2016).
23. Yoon, H. et al. Repression of microbial arsenite uptake and methylation by dissolved organic carbon. Environ. Sci. Technol. Lett. 11, 838–844 (2024).
24. Chen, S.-Y. et al. Development of a Highly Sensitive Whole-Cell Biosensor for Arsenite Detection through Engineered Promoter Modifications. ACS Synth. Biol. 8, 2295–2302 (2019).
25. Kalvapalle, P. B., Sridhar, S., Silberg, J. J. & Stadler, L. B. Long-duration environmental biosensing by recording analyte detection in DNA using recombinase memory. Appl. Environ. Microbiol. 90, e0236323 (2024).
26. Akboğa, D., Saltepe, B., Bozkurt, E. U. & Şeker, U. Ö. Ş. A Recombinase-Based Genetic Circuit for Heavy Metal Monitoring. Biosensors 12, (2022).
27. Kremers, G.-J., Goedhart, J., van Munster, E. B. & Gadella, T. W. J., Jr. Cyan and yellow super

fluorescent proteins with improved brightness, protein folding, and FRET Förster radius. Biochemistry 45, 6570–6580 (2006).
28. Li, C. et al. FastCloning: a highly simplified, purification-free, sequence- and ligation-independent PCR cloning method. BMC Biotechnol. 11, 92 (2011).
29. Gibson, D. G. et al. Enzymatic assembly of DNA molecules up to several hundred kilobases. Nat. Methods 6, 343–345 (2009).
30. Sibley, M. H. & Raleigh, E. A. A versatile element for gene addition in bacterial chromosomes. Nucleic Acids Res. 40, e19 (2012).
31. Pothier, M. P., Hinz, A. J. & Poulain, A. J. Insights Into Arsenite and Arsenate Uptake Pathways Using a Whole Cell Biosensor. Front. Microbiol. 9, 2310 (2018).
32. Yoon, H. et al. Time-Dependent Biosensor Fluorescence as a Measure of Bacterial Arsenic Uptake Kinetics and Its Inhibition by Dissolved Organic Matter. Appl. Environ. Microbiol. 88, e0089122 (2022).

SUPPORTING INFORMATION

Table S1 | Growth rates measured for each experiment shown in Fig. 2.
Growth rates are computed for each technical replicate by fitting a linear model to the plate reader ln(OD600) data versus time, during the exponential growth phase. We report the average growth rate across three technical replicates. We report the p-value of Welch's t-test for each treatment. Fits were performed using data points that fell within the same range of OD values, for each strain. Growth rates reported in the last four rows were measured in a separate experiment, where we tested the reporter with 1 mM of cuminic acid. We observe that using such a high concentration of inducer results in a growth rate statistically significantly lower with respect to the reference strain.

Strain	Cuminic acid concentration	Growth rate (mean ± SEM)	p-value
bAG56	0 μM	1.01 ± 0.01 h^{-1}	
bAG56	10 μM	1.014 ± 0.007 h^{-1}	0.61
bAG56	50 μM	0.95 ± 0.02 h^{-1}	0.09
bAG56	100 μM	0.97 ± 0.02 h^{-1}	0.16
bEG39	0 μM	1.12 ± 0.01 h^{-1}	
bEG39	2 μM	1.04 ± 0.08 h^{-1}	0.41
bEG39	4 μM	1.12 ± 0.02 h^{-1}	0.98
bEG39	10 μM	1.12 ± 0.02 h^{-1}	0.97
bEG36	0 μM	1.28 ± 0.03 h^{-1}	
bEG36	3 μM	1.26 ± 0.02 h^{-1}	0.53
bEG36	5 μM	1.23 ± 0.03 h^{-1}	0.32
bEG36	10 μM	1.21 ± 0.04 h^{-1}	0.20
bEG57	0 μM	1.20 ± 0.05 h^{-1}	
bEG57	3 μM	1.13 ± 0.04 h^{-1}	0.30
bEG57	5 μM	1.22 ± 0.02 h^{-1}	0.76
bEG57	10 μM	1.1 ± 0.1 h^{-1}	0.30
bAG56	0 μM	1.21 ± 0.02 h^{-1}	

bAG56	50 µM	1.19 ± 0.02 h^{-1}	0.64
bAG56	100 µM	1.16 ± 0.02 h^{-1}	0.12
bAG56	1000 µM	1.07 ± 0.02 h^{-1}	0.006*

Table S2 | P-values for the arsenite biosensors sensitivity assay (Fig. 4).
Reported are individual Welch's t-test p-values comparing treatments within biological replicates, as well as the combined p-value (across biological replicates) obtained with Fisher's method.

	Recombinase-based biosensor (pEG69)			
Comparison	**Exp. 1**	**Exp. 2**	**Exp. 3**	**Combined**
0 - 15 nM	0.24	2.4×10^{-2}	1.1×10^{-4}	7.4×10^{-5}
15 - 30 nM	2.0×10^{-3}	6×10^{-5}	4.1×10^{-3}	1.5×10^{-8}
30 - 45 nM	5.3×10^{-4}	4.9×10^{-4}	6.7×10^{-4}	4.8×10^{-8}
45 - 60 nM	1.1×10^{-4}	4.8×10^{-4}	4.2×10^{-3}	5.7×10^{-8}

	Transcription-based biosensor (pEG78)			
Comparison	**Exp. 1**	**Exp. 2**	**Exp. 3**	**Combined**
0 - 15 nM	6.4×10^{-2}	2.0×10^{-4}	2.4×10^{-2}	3.9×10^{-5}
15 - 30 nM	1.2×10^{-2}	0.11	8.8×10^{-2}	5.9×10^{-3}
30 - 45 nM	5.9×10^{-4}	7.3×10^{-3}	0.36	1.6×10^{-4}
45 - 60 nM	6.4×10^{-2}	0.36	0.38	0.15

Table S3 | Oligos used in this study.

Oligo	**Sequence $5' \rightarrow 3'$**	**Description**
oAG90	atcagaccggaaagcacatc	FWD primer on pAJM.657 to include *cymR*^{AM} and insert the *cre-lox* construct via Fastcloning
oAG91	AGGACGAAACAGCCTCTAC	REV primer on pAJM.657 to include *cymR*^{AM} and insert the *cre-lox* construct via Fastcloning
oAG92	tgctttccggtctgatgaAAGAGGGGAAATACTAGA	FWD primer on Addgene plasmid #62730 to amplify *cre*
oAG93	tcgtcattgatcaaagcTTAAGCTACTAAAGCGTAGTTTT	REV primer on Addgene plasmid #62730 to amplify *cre*
oAG94	acgctttagtagcttaaGCTTTGATCAATGACGAACAATAAGG	FWD primer for Fastcloning - anneal on Twist Bioscience *lox* sites sequence
oAG95	gaggctgtttcgtcctTCCTTCTTAAAATAACTTCGTATAATGTATGC	REV primer for Fastcloning - anneal on Twist Bioscience *lox* sites sequence
oAG129	ccttttcggcatcgccctaaaattcggAGAGGGACACGGCGAAATAA	FWD primer on pEG36 to replace *W4p* with *rpsLp*
oAG130	agggcgatgccgaaaaggtgtcaagaaatataCCAGAAACAAAAAAAGGCCGCG	REV primer on pEG36 to replace *W4p* with *rpsLp*

oAG131	aaagaggagaaatactagATGGTGAGCAAGGGCGAGGA	FWD primer on pEG36 to introduce strong RBS upstream FP
oAG132	ctagtatttctcctctttGAGGCTGTTTCGTCCTTCCTTCT	REV primer on pEG36 to introduce strong RBS upstream FP
oEG96	gattcaggaatacagaGATAAGGATCCTAATTGGT	FWD primer to delete *cymR*^{AM}
oEG97	tctgtattcctgaatcCATTGGACCAAAACGAA	REV primer to delete *cymR*^{AM}
oEG98	tatagcatACATTATACGAAGTTATCAAACGCATG	FWD primer on pAG56 to replace *lox511* with *loxP*
oEG99	tataatgtatgCTATACGAAGTTATTTCGCCGTGT	REV primer on pAG56 to replace *lox511* with *loxP*
oEG89	tattttaattaaTTAGAAAAACTCATCGAGCATCA	FWD primer on pEG55 to amplify reporter and add PacI restriction site
oEG123	attactcgagAGTGCCAACATAGTAAG	REV primer on pEG55 to amplify reporter and add PacI restriction site
oEG48	CCTGATTTATGGCGCGAAAG	FWD primer in *cre* for colony PCR
oEG102	CTGAACTTGTGGCCGTTTAC	REV primer in *eyfp* for colony PCR
oEG116	CCGTATGTTGCATCACCTTC	REV primer in *syfp2* for colony PCR
oAG70	AATCTGTAACGTTCCGGGTTC	FWD primer downstream *attTn7* to verify integration in the chromosome
oEG103	CGGTGGTACGCATAACTTTC	REV primer downstream *attTn7* to verify integration in the chromosome
oEG112	agaaatactagATGAGTAAAGGAGAA	FWD primer on bAG10 to amplify *syfp2*
oEG113	tatttgctcaGATTTGTCCTACTCA	REV primer on bAG10 to amplify *syfp2* + its terminator
oEG114	aggacaaatcTGAGCAAATATTTTATCTGAGG	FWD primer on pEG36 to remove *eyfp*
oEG115	ctttactCATCTAGTATTTCTCCTCTTTG	REV primer on pEG36 to remove *eyfp*
oEG150	ttttctccttcattaCAGTCACGACGTTGT	FWD on pMP01 to remove second origin of replication
oEG151	taatgaaggagaaaaGTCAGGTGGCACTTT	REV on pMP01 to remove second origin of replication
oEG144	gagtaggacaaatcGTTTGCGTATTGGGC	FWD on pMP01 to remove *mCherry*
oEG145	tccggtgacagctaGTGATGGTGATGGTG	REV on pMP01 to remove *mCherry*
oEG146	accatcaccatcacTAGCTGTCACCGGAT	FWD primer on pEG55 upstream *cymRCp* to insert downstream of *arsR*
oEG147	CCCAATACGCAAACGATTTGTCCTACTCA	REV primer on pEG55 in *syfp2* terminator
oEG148	accatcaccatcacGAAACAGCCTCAAAG	FWD primer on pEG55 upstream strong RBS + *syfp2*
oEG172	ggcgttaattaaACGAAAACTCACGTTAAG	FWD primer to add PacI restriction site for

		cloning on low copy number plasmid
oEG173	atttctcgagCAATACGCAAACGATTTGTC	REV primer to add XhoI restriction site for cloning on low copy number plasmid

Additional notes for the data analysis

Cuminic acid sensitive reporter response characterization

Fig. 2D data: The first measurement time points taken by the plate reader after pipette sampling were excluded from the analyses due to lid condensation that interfered with the measurement.

Fig. 3 data: Each treatment in Fig. 3 started with 12 technical replicates, to be used partly for flow-cytometry and partly for colony-PCR as follows. Replicates 1-3 were analyzed with flow-cytometry at time t_1 and then pooled for the t_1 colony-PCR measurement. Replicates 4-6 were analyzed with flow-cytometry at time t_2 and then pooled for the t_2 colony-PCR measurement. Replicates 7-9 were analyzed with flow-cytometry at time t_3 and then pooled for the t_3 colony-PCR measurement. Replicates 10-12 were analyzed with flow-cytometry at each time step and then pooled for the final t_4 colony-PCR measurement. Therefore, data points in Fig. 3A-B at times t_1 to t_3 are means computed across 6 technical replicates (the 3 replicates specific to that time point, plus replicates 10-12), whereas time t_4 is the mean across the 3 technical replicates 10-12. The following technical replicates were excluded from the analysis, due to technical errors, as detailed below:

For the plasmid reporter pEG36 (Fig. 3A):
- One of the three technical replicates induced with 10 μM of cuminic acid is missing from the t_4 measurement due to a pipetting error.

For the chromosomal reporter bEG57 (Fig. 3B):
- At t_2, data for 2 technical replicates with inducer concentration of 4 μM are missing from the flow-cytometry data collection.
- At t_3, one pipetting error occurred during flow-cytometry sampling of one technical replicate induced with 10 μM of cuminic acid.

Arsenic sensitive reporter response characterization

The following samples were excluded from the analysis (Fig. 4):

Biological replicate 2 (orange points):
- Cross-contamination between one technical replicate of pEG68 and one technical replicate of pEG78 without arsenite in one well. These two technical replicates were excluded from the analysis, and thus only 4 technical replicates remain. One technical replicate of pEG78 (Fig.4B) treated with 15 nM arsenite did not grow and was thus excluded from the analysis.

Biological replicate 3 (green points):
- One technical replicate of pEG78 (Fig.4B) treated with 45 nM arsenite did not grow and was thus excluded from the analysis.